

Drawing of Microstructured Optical Fibres: Modelling and Stability

Rodney Dharma, Andres E. Rubiano, and Yvonne M. Stokes *

1 Introduction

Professor Yvonne Stokes delivered an insightful seminar titled “Drawing of Microstructured Optical Fibres: Modelling & Stability” at the MATRIX Instabilities of Porous Media Workshop. Her talk focused on the mathematical modelling and stability analysis of microstructured optical fibres (MOFs), which are crucial components in modern optical communication and sensing technologies. For more details on this work, please see [8, 9, 10].

The talk began with an introduction to optical fibres. These are cylindrical fibres typically made of glass, with diameters of around $150\ \mu\text{m}$. They are used to transmit light. Conventional optical fibre consists of a solid glass core (the fibre) surrounded by a cladding. To guide light there must be a change in refractive index at the core-cladding interface for internal reflection of light. Good thermo-mechanical coupling between the core and the surrounding cladding is also necessary. In contrast, only a single material is used for microstructured optical fibres (MOFs) through which air channels run along the length of the fibre. These air channels have diameters around the wavelength of light. They provide the necessary change in the refractive index to guide light along the core. The seemingly limitless number of possible

Rodney Dharma
The University of Melbourne, Grattan Street, Parkville Victoria 3010, Australia
e-mail: dharmar@student.unimelb.edu.au

Andres E. Rubiano
Monash University, 9 Rainforest Walk, Clayton, Victoria 3163, Australia
e-mail: andres.rubianomartinez@monash.edu

Yvonne M. Stokes
The University of Adelaide, North Terrace, Adelaide, South Australia 5001, Australia
e-mail: yvonne.stokes@adelaide.edu.au

* These lecture notes are based on a lecture delivered by Prof. Yvonne Stokes (University of Adelaide) at the Matrix Workshop *Instabilities in Porous Media*, April 3-23, 2024.

channel arrangements and shapes has led to a large expansion in the uses for optical fibres. MOFS have applications in technologies for telecommunication, chemical/biological sensing, and medical imaging.

There are two stages to MOF fabrication: (1) manufacture of the preform, and (2) drawing of the preform into the fibre. Devices for both of these processes are shown in Fig. 1. Preform extrusion involves pushing a billet of heated glass through a die as seen in Fig. 1(a). The resulting glass preform is then drawn to a fibre in a draw tower as depicted in Fig. 1(b). The talk focused on the latter stage of MOF fabrication: modelling the drawing of the preform fibre.

As a preform is drawn to a fibre, there will be deformation of the preform geometry due to stretching, surface tension and, if applied, pressure in the air channels. Hence, the microstructure in the resulting MOF may not be the desired shape. This leads to two fundamental questions: (1) What will be the deformation from preform to fibre? (2) How to make the desired fibre? The former is known as the forward problem (given a known initial shape of the preform, we want to know the shape of the fibre), and the latter is the inverse problem (given the desired shape of the fibre, what will be the required shape of the preform).

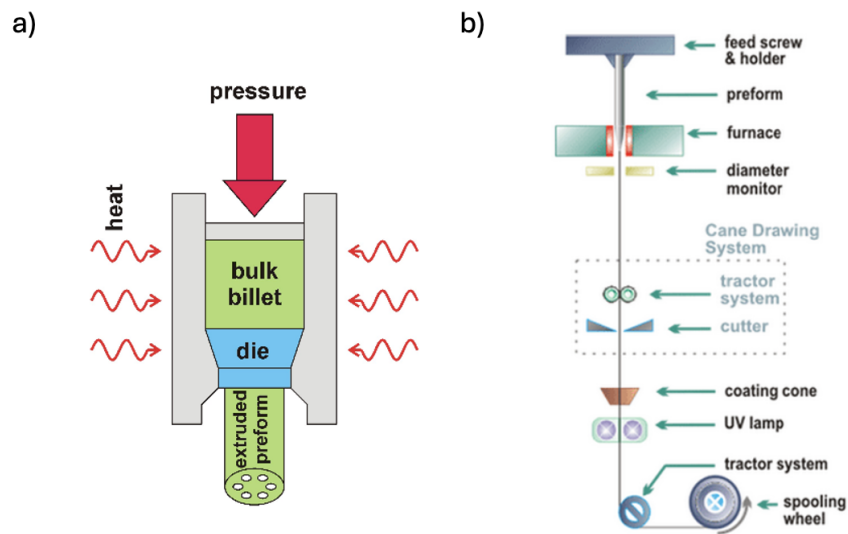


Fig. 1 (a) Preform extrusion through a die; diagram reproduced from [3]. Fibre drawing from a preform; diagram reproduced from [1].

2 Modelling the steady-state fibre drawing process

As a way to study this problem, Stokes et. al. [8] mathematically modelled the drawing process. The full problem is described by the Navier-Stokes equations with boundary conditions on free surfaces that balance viscous stress in the fluid with surface tension and that describe the fluid moving with the boundary (the kinematic condition). In addition, the heat equation describes convective and radiative heat transfer in the glass and through the free surfaces. The inlet and outlet velocities, U_{in} and U_{out} , and the inlet temperature θ_{in} and geometry are prescribed. Also, assume a zero temperature gradient at the outlet, $\theta_x = 0$, where x is in the direction of the stretching. Figure 2 shows a schematic diagram of the problem and the associated coordinate system. FIG 2(a) shows the neck down region, while Fig. 2(b) gives an example fibre cross-section. Note that the external boundary of the cross-section is denoted $G^{(0)}(x) = 0$ and the N internal boundaries are denoted $G^{(i)}(x) = 0$, $i = 1, 2, \dots, N$.

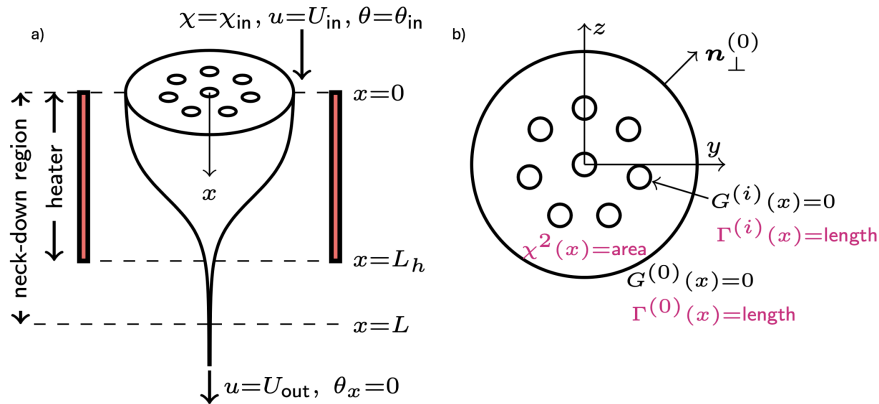


Fig. 2 (a) Schematic diagram for the neck down region showing the coordinate axis x . (b) An example of cross-sectional geometry of the fibre at axial position x . Both diagrams are taken from lecture slides provided by Prof. Yvonne Stokes.

For modelling purposes, the fact that $\epsilon = \chi_{in}/L \ll 1$ can be exploited, where χ_{in} is the cross-sectional area at the inlet, and L is the neck-down length. This allows us to derive a simpler asymptotic model.

The dimensionless steady leading-order model is

$$u\chi^2 = 1, \quad (1)$$

$$\text{Re}\chi^2 \left(u \frac{du}{dx} \right) = \frac{d}{dx} \left(3\mu(\theta)\chi^2 \frac{du}{dx} \right) + \frac{1}{2\text{Ca}} \frac{d\Gamma}{dx}, \quad (2)$$

$$u \frac{d\theta}{dx} = \frac{1}{\text{Pe}\chi^2} \frac{d}{dx} \left(\chi^2 \frac{d\theta}{dx} \right) - \frac{\Gamma^{(0)}}{\text{Ca}\chi^2} (\mathcal{H}_C f_C(\theta) + \mathcal{H}_R f_R(\theta, x)), \quad (3)$$

where $\chi^2(x, t)$ is the cross-sectional area, $u(x, t)$ is the axial velocity, $\Gamma(x)$ is the total cross-sectional boundary length, $\Gamma^{(0)}(x)$ is the cross-sectional external boundary length, and $\mu(\theta)$ is the viscosity as a function of θ . It is here assumed that the surface tension does not depend on temperature and is constant. The boundary conditions of the problem are $\chi(0, t) = 1$, $u(0, t) = 1$, $u(1, t) = D = U_{\text{out}}/U_{\text{in}}$, while the parameters of the problem are the Reynolds number Re , capillary number Ca , Peclet number Pe , radiative heat transfer coefficient \mathcal{H}_R , and dimensionless convective heat transfer \mathcal{H}_C [8, 9]. Note that the functions f_R and f_C are defined as

$$f_C(\theta) = \left(1 - \frac{\theta_{\text{in}}}{\theta_{\text{hot}}}\right)\theta + \frac{\theta_{\text{in}}}{\theta_{\text{hot}}} - \frac{\theta_a}{\theta_{\text{hot}}}, \quad (4)$$

$$f_R(\theta, x) = \begin{cases} \left(\theta + \frac{\theta_{\text{in}}}{\theta_{\text{hot}}}(1 - \theta)\right)^4 - \left(\frac{\theta_h(x)}{\theta_{\text{hot}}}\right)^4, & \text{if } 0 \leq x \leq l \\ \left(\theta + \frac{\theta_{\text{in}}}{\theta_{\text{hot}}}(1 - \theta)\right)^4 - \left(\frac{\theta_h(x)}{\theta_a}\right)^4, & \text{if } l < x \leq 1. \end{cases} \quad (5)$$

Here $\theta_{\text{in}}/\theta_{\text{hot}}$, $\theta_a/\theta_{\text{hot}}$, and $\theta_h(x)/\theta_{\text{hot}}$ are the input glass, ambient air and heater temperature scaled with θ_{hot} , the maximum temperature within the glass should it be simply placed in the heater and left to reach equilibrium [9]. The constant $l = L_h/L$ is the dimensionless length of the heater.

The quantities $\Gamma(x)$ and $\Gamma^{(0)}(x)$ are given by solution of a 2D Stokes flow problem in the cross-section of the fibre. Writing the pressure and velocity in the cross-section as

$$p = p_z + \frac{1}{\text{Ca}\chi} \tilde{p}, \quad (v, w) = (v_z, w_z) + \frac{1}{\text{Ca}\mu(\theta)} (\tilde{v}, \tilde{w}),$$

re-scaling quantities with $\chi(x)$, and utilising the transformation from x to τ ,

$$\frac{d\tau}{dx} = \frac{\chi}{\text{Ca}\mu(\theta)}, \quad (6)$$

where $\tau = 0$ at $x = 0$, gives the cross-plane model as a classical 2D free-boundary Stokes-flow problem in a domain of unit area driven by unit surface tension and pressure P in the air channels [8, 9]. For brevity, please see [8] and [9] for more details.

Assuming $\text{Re} \ll 1, \text{Pe} \gg 1$ (valid for fibre drawing) and writing (1) in terms of τ gives

$$\frac{d\chi}{d\tau} - \frac{1}{12}\chi\tilde{\Gamma} = -CaT, \tag{7}$$

$$\frac{d\theta}{d\tau} = -\frac{\mu(\theta)\tilde{\Gamma}^{(0)}}{Ca}(\mathcal{H}_R f_R + \mathcal{H}_C f_C), \tag{8}$$

$$\frac{dx}{d\tau} = \frac{Ca\mu(\theta)}{\chi}, \tag{9}$$

with boundary conditions $\chi(0) = 1$, $\theta(0) = 0$, $x(0) = 0$, $\chi(\tau_{\text{end}}) = 1/\sqrt{D}$ and $x(\tau_{\text{end}}) = 1$. A notable feature of the model is that it can be solved for $\chi(\tau)$ for chosen tension T and pressure in the air channels P without solving for temperature. However, the location x for each τ depends on temperature via the viscosity $\mu(\theta)$. In [8] it was found that the tension, T , can be used as a proxy for the temperature (without solving for the temperature) if only the final fibre geometry is important since the tension determines the harmonic mean of μ and the final fibre geometry [8, 9].

The forward problem can be solved for any cross-plane geometry, for example using the complex variable method of [2]. The inverse problem, however, is ill-posed, since different preforms can yield indistinguishable fibres. This means that the inverse problem is solvable provided one constrains the geometry of the preform to only a subset of the possible configurations.

3 Draw stability

Matovich and Pearson [5] first showed that the drawing of a thin solid thread under isothermal conditions and with negligible inertia and surface tension is stable for draw ratios $D < D_{\text{crit}} \approx 20.21$. For larger draw ratios, there is instability known as draw resonance. However, draw stability can be affected by inertia, temperature, surface tension, air channels in the fibre, and pressure in these channels. It has been shown that for the drawing of solid fibres (with no air channels), inertia has a stabilising effect while surface tension is destabilising [7]. However, the question of how air channels affect this stability, posed in [4], has only recently been answered [10]. The question ‘‘How do one or more air channels affect stability?’’ was considered in the talk for the case of isothermal drawing with no pressurisation of the air channels, using a linear stability analysis.

For this, the dimensionless unsteady leading-order model was written, in the form

$$\text{Re}\chi^2 \left(\frac{\partial u}{\partial t} + u \frac{du}{dx} \right) = \frac{d}{dx} \left(3\chi^2 \frac{du}{dx} \right) + \frac{1}{2Ca} \frac{d\chi\tilde{\Gamma}}{dx}, \tag{10}$$

$$\frac{\partial}{\partial t}(\chi^2) + \frac{\partial}{\partial x}(u\chi^2) = 0, \tag{11}$$

$$\frac{\partial \tau}{\partial t} + u \frac{\partial \tau}{\partial x} = \frac{1}{\chi Ca}, \tag{12}$$

where $\chi(x, t)\tilde{\Gamma}(\tau)$ is the total cross-sectional boundary length, and $\tilde{\Gamma}(\tau)$ is the re-scaled cross-sectional boundary length for the 2D Stokes-flow problem in the cross section. All other parameters retain the same definition as previously mentioned for the steady case.

Writing $u(x, t) = u_0(x) + \exp(\lambda t)\tilde{u}_0(x)$ where $u_0(x)$ is the steady-state velocity and the second term is a small perturbation, with similar expressions for $\chi(x, t)$ and $\tau(x, t)$, and substituting these expressions into the model yields an eigenvalue problem for the growth rate λ . The solution of this problem for λ with the largest real part shows drawing to be stable if the real part $Re(\lambda) < 0$ and unstable if $Re(\lambda) > 0$. For given parameters Re , Ca , and geometry as represented by the boundary length $\tilde{\Gamma}(\tau)$ the critical draw ratio D_{crit} was determined such that $Re(\lambda) = 0$.

It was found that the critical draw ratio, D_{crit} , is smaller for a tube than a solid fibre, (i.e. that an air channel destabilises fibre drawing). Moreover, D_{crit} decreases as the initial size of the air channel increases, (i.e. as $\tilde{\Gamma}(0)$ increases). Moreover it was shown that, no matter what the geometry of the air channels, a longer initial boundary length $\tilde{\Gamma}(0)$ destabilises fibre drawing. It was also shown that surface tension destabilises drawing (i.e., as Ca decreases, so does D_{crit}). This is in contrast with inertia, where increasing the Reynolds number, Re , will increase D_{crit} , thereby stabilising the system.

Adding to the complexity of this problem, although pressurisation of air channels and cooling of the fibre was not included in the model described in the talk, results were shown from [6] revealing that cooling stabilises in the absence of pressure, that pressure has no effect on stability in the absence of surface tension and cooling, and that the effect of combined pressure and cooling depends on their relative strengths and hole size. For small inlet hole sizes, pressure will stabilise because it acts to increase the hole size and external boundary length, and so enhances the cooling of the fibre. Conversely, for a large inlet hole, pressure does not significantly affect cooling, and destabilises drawing.

The overall analysis demonstrated in this talk, highlights the complexity of the stability landscape in this problem, showing that stability is highly sensitive to the initial boundary length. Moreover, the mathematical modelling developed provided an excellent understanding of fibre drawing and its stability. Importantly an open problem posed in [4] was shown to be solved.

References

1. Max Planck Institute for the science of light: Fibre fabrication. URL <https://mpl.mpg.de/research-at-mpl/technology-development-service-units/tdsu-fibre-fabrication-glass-studio/research/fibre-fabrication/stack-and-draw>
2. Crowdy, D.: Viscous sintering of unimodal and bimodal cylindrical packings with shrinking pores. *European Journal of Applied Mathematics* **14**, 421–445 (2003). DOI 10.1017/s095679250300514x
3. Ebdorff-Heidepriem, H., Monro, T.M.: Extrusion of complex preforms for microstructured optical fibers. *Optics Express* **15**, 15,086 (2007). DOI 10.1364/oe.15.015086

4. Fitt, A., Furusawa, K., Monro, T., Please, C., Richardson, D.: The mathematical modelling of capillary drawing for holey fibre manufacture. *Journal of Engineering Mathematics* **43**, 201–227 (2002). DOI 10.1023/a:1020328606157
5. Matovich, M.A., Pearson, J.R.A.: Spinning a molten threadline. steady-state isothermal viscous flows. *Industrial & Engineering Chemistry Fundamentals* **8**, 512–520 (1969). DOI 10.1021/i160031a023
6. Papri, N.N., Wylie, J.J., Stokes, Y.M.: Drawing of hollow fibres: effects of surface tension, cooling, internal pressurisation and inertia on steady states and stability. *Journal of Fluid Mechanics* (2024, submitted)
7. Schultz, W.W., Davis, S.H.: Effects of boundary conditions on the stability of slender viscous fibers. *Journal of Applied Mechanics* **51**, 1–5 (1984). DOI 10.1115/1.3167573
8. Stokes, Y.M., Buchak, P., Crowdy, D.G., Ebendorff-Heidepriem, H.: Drawing of microstructured fibres: circular and non-circular tubes. *Journal of Fluid Mechanics* **755**, 176–203 (2014). DOI 10.1017/jfm.2014.408
9. Stokes, Y.M., Wylie, J.J., Chen, M.J.: Coupled fluid and energy flow in fabrication of microstructured optical fibres. *Journal of Fluid Mechanics* **874**, 548–572 (2019). DOI 10.1017/jfm.2019.466
10. Wylie, J.J., Papri, N.N., Stokes, Y.M., He, D.: Stability of drawing of microstructured optical fibres. *Journal of Fluid Mechanics* **962** (2023). DOI 10.1017/jfm.2023.267